Indian Journal of Engineering & Materials Sciences
Vol. 27, April 2020, pp. 246-255

Optimization and investigation of process parameters in single point incremental forming

Ajay Kumar[a *] & Vishal Gulati[b]

[a]Department of Mechanical Engineering,
Faculty of Engineering and Technology, Shree Guru Gobind Singh Tricentenary University, Gurugram, 122505, Haryana, India.
[b]Department of Mechanical Engineering,
Guru Jambheshwar University of Science & Technology, Hisar 125001, Haryana, India.

Received : 28 June 2017 ; Accepted : 13 August 2018

Single point incremental forming (SPIF) process is an innovative and dies-less forming technique to produce various useful shapes for small batch size economically. This process exempts expensive and complex tooling which is used in traditional sheet forming processes. Study of forming force and thickness reduction of the components formed by SPIF process would help the process engineers to provide some guidelines regarding the implementations of this process to mainstream of manufacturing industries. In this work, seven impact factors of this process have been exploited to optimize SPIF process using Taguchi method as a design of experiment (DoE) technique. The objective of current work is to optimize the forming forces and thickness reduction of the formed conical frustums for a given set of factors for operation sustainability. The predictive models have also been generated for estimating optimal characteristics of the process. The predictive model estimated the response characteristics of the SPIF process effectively and accurately.

Keywords: SPIF, Optimization, Forming force, Thickness reduction, AA2014, Tool path

1 Introduction

Manufacturing processes for giving desired shape and size to raw material, by permanently deforming it using force, pressure or stresses like compression, tension, shear or their combinations, are known as forming processes. The material is deformed to the desired shape and size with almost no wastage. Sheet material forming started in early days of humanity evolution and is a sub-class of material forming processes. Products made from sheet-material are all around us and are widely used. An extensive range of products are manufactured with the use of sheet materials such as parts of automobiles, aircrafts, agriculture equipment *etc*.[1]. In conventional forming processes the required forming forces to produce deformation are quiet high and formability of formed components is lower[2].

Conventional sheet-forming processes require custom designed expensive tooling systems (punch and die) for each component to be manufactured by sheet forming[3]. If only one or few components are to be manufactured, conventional methods are highly uneconomical.

Hence, a forming process that is capable of forming the components in batch size can be patronizing route to produce different requirements of production industry. Incremental Sheet Forming (ISF) process possesses the possibilities to satisfy such a demand of manufacturing industry[4]. Single Point Incremental Forming (SPIF) is the important variant of ISF process which is also known as negative incremental forming[5].

SPIF technique is characterized by progressively applying plastic deformation to sheet material, with a forming tool that is maneuvered by a Computer Numerical Control (CNC) action on a milling machine or by an industrial robot[6-7]. The forming tool performs the incremental localized deformation of sheet while moving along a predefined trajectory, descending a small step in each contour[8]. The schematic of SPIF is illustrated by Fig. 1.

Stretching conditions prevails in SPIF process and significant thickness reduction of sheets occurs. Maximum allowable thickness reduction of sheet is an important response of SPIF process[9]. Fracture limit is greatly affected by thickness reduction limit of the material that further decides precision of the process. The selection of forming hardware for SPIF process is controlled by required forming forces and accuracy. Similarly, the excessive reduction in thickness during

*Corresponding author (E-mail: ajay.kumar30886@gmail.com)

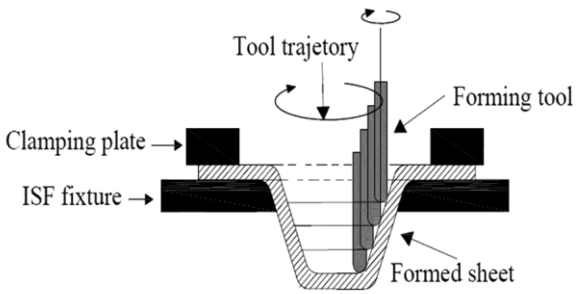

Fig. 1 — Schematic of single point incremental forming.

forming process results in the fracture of sheet metal. Maximum allowable thinning of sheet is an important response of this die-less process. It is mandatory for a process engineer to know the allowable thinning of sheet metal without fracture.

As compared to traditional forming processes, SPIF possesses greater formability due to localized deformation induced during tool movement over the surface of sheet material**.** Since, volume of the blank is constant, therefore, material should be formed at the expense of its thickness and final sheet thickness is generally obtained by Eq. (1)[10].

$$T_f = T_o \cos \alpha \qquad \dots (1)$$

where, T_f is the final thickness, T_o is the original thickness and α is the forming angle.

Thicker sheets are expected to have higher formability[11]. The thinning of the sheet at a depth and slop at which failure occurs is known as thinning limit. Estimation of thickness reduction is required to ensure the safe forming of the components without fracture. Various researchers have investigated impact of various process variables on forming forces and thickness reduction during SPIF process. Duflou *et al.*[12] investigated the effectiveness of local and dynamic heating as a means of reducing forces in SPIF process. A gradual drop in the forming forces was observed at elevated temperatures. Aerens *et al.*[13] developed a theoretical model for predicting forming forces for various materials using different input parameters. Oleksik *et al.*[14] found that sheet thickness was the most influencing input factor. Bagudanch *et al.*[15] and Centeno *et al.*[16] investigated impact of tool radius for PVC and the forming forces increased with the rise in tool radius. Kumar *et al.*[17] studied the impact of tool diameter on the axial peak forming forces for different sheet thickness and observe the same trend. Kumar and Gulati[18] optimized the various impact factors and found that sheet thickness is most influencing factor amongst the investigated factors. Petek *et al.*[19] observed that sheet material was failed when no lubricant was used during forming process. Duflou *et al.*[20] compared forming force for conical and pyramid frustums, and observed that maximum axial forming force is independent of these two part geometries.

Some studies[21-26] have also been conducting towards analysis of thickness distribution and thinning limits. Ambrogio *et al.*[21] and Young & Jeswiet[22] investigated thickness reduction of the formed components and found that cosine law holds well. Skjoedt *et al.*[23] formed the cup-shaped geometry and found that thickness reduction increased when wall angle was enhanced. Hussain and Gao[24] investigated effects of feed rate and forming angle on thickness reduction of the formed parts. They found that constant wall angle resulted in the higher thinning limit of the formed parts. Gulati *et al.*[25] contributed towards optimization of process parameters and observed that higher formability can be achieved by increasing spindle speed and sheet thickness. Lubrication was found the most influencing factor and grease produced better formability. Kurra *et al.*[26] investigated thickness distribution on EDD steel sheets. Thickness distribution was also analyzed with LS-DYNA code and a comparison was made with experimental results. Experimental and simulation results of thickness measurements were found in good correlation. Results showed that EDD sheets could be formed without fracture up to 75% of thickness reduction.

It has been realized from the literature survey that very limited work has been executed towards investigation and optimization of input factors in SPIF on forming force and thickness reduction. SPIF is characterized by different input parameters and responses. Different input parameters affecting the process can be categorized among material parameters, geometrical parameters, and process parameters. Material parameters (Young modulus, work hardening exponent, the anisotropy of material) and geometrical parameters (part shape, wall angle and sheet thickness) are hardly modified due to many constraints of the process. On the other hand, process designer has the choice of altering process parameters (step size, spindle speed, feed rate, punch diameter, lubrication, tool path etc). Study of forming forces and thickness reduction of the components formed by SPIF process would help the process engineers to provide some guidelines regarding the implementations of this process to mainstream of manufacturing industries. Therefore, optimization and study of impact factors is quiet important in this die-less process. Experimental investigation and optimization of impact factors would help a production engineer to develop the precise model of SPIF process. In addition, it has also been observed from literature review that aluminum alloy AA2014 is still unexplored in SPIF process in terms of optimizing the process. This alloy has wide range of applications in aerospace and military sectors.

The current study points towards systematic investigation of input variables on AA2014 alloy using Taguchi Method (TM) as a DOE and optimizing technique in order to achieve optimal conditions for forming forces and thickness reduction. Effects of seven input factors *viz*. sheet thickness, radius of tool, tool path or tool trajectory, step size, feed rate, lubrication and tool rotation have been investigated on forming forces and thickness reduction of the formed components. Main agenda of this study is to find optimal range of impact factors for minimal forming force and thickness reduction on formed sheet experimentally and to optimize the impact factors using TM and the results are statistically processed through the ANOVA technique. Hence, it is an important aspect for experimental investigation and optimization of input variables for SPIF technique on AA2014 sheets.

2 Materials and Methods

2.1 Process description and tooling set-up

SPIF process includes the movement of forming tool on sheet material by NC action on a CNC milling machine and to produce local deformation layers by layers to follow a predetermined path. Sheets of AA2014 alloy of size 250×250 mm^2 was taken into account. Table 1 depicts the compositions of AA2014 alloy. Hemispherical shaped forming tools (Fig. 2), made of K110 steel, of three different diameters (16, 18, and 20 mm) have been studied. CAD model of truncated shape having 130 mm upper diameter and 65^o wall angle was generated with the help of CATIA-V5 software. Then the CAD model was imported to MASTER-CAM9 software in order to construct numerical instructions for tool path. All the experiments have been performed on a vertical machining centre (VMC2216XV-Bridgeport) equipped with FANUC-2Li controller (Fig. 3). The sheet was clamped in the SPIF fixture as shown in Fig. 4. In this work, three types of lubricants (coolant, mineral oil, and grease) have been investigated during SPIF process. Figure 4 represents experimental set-up for SPIF process.

Table 1 — Chemical compositions of AA2014 alloy.

Al	Chemical composition (weight %)							
	Cr	Cu	Fe	Mg	Mn	Si	Ti	Zn
Balance	0.10	4.50	0.70	0.60	0.80	0.70	0.10	0.25

Forming tool trajectory is an important factor that determines the preciseness and accuracy of the formed parts during SPIF process[27-28]. In this work, profile and helical tool trajectories (Fig. 5) are executed to produce the components. These tool trajectories are well described by Kumar *et al.*[5, 18].

2.2 Measurement of forming force and thickness reduction

A load dynamometer and a data logger system were employed to record the force values. Table 2 shows the characteristics of the data logger system used in this study. A digital micrometer having a least count 0.01 mm has been used for measuring thickness reduction of the formed components. For the ease of measurement, the formed components were sectioned

Fig. 2 — K110 steel tool of 20 mm diameter.

Fig. 3 — Machine tool used for SPIF tests.

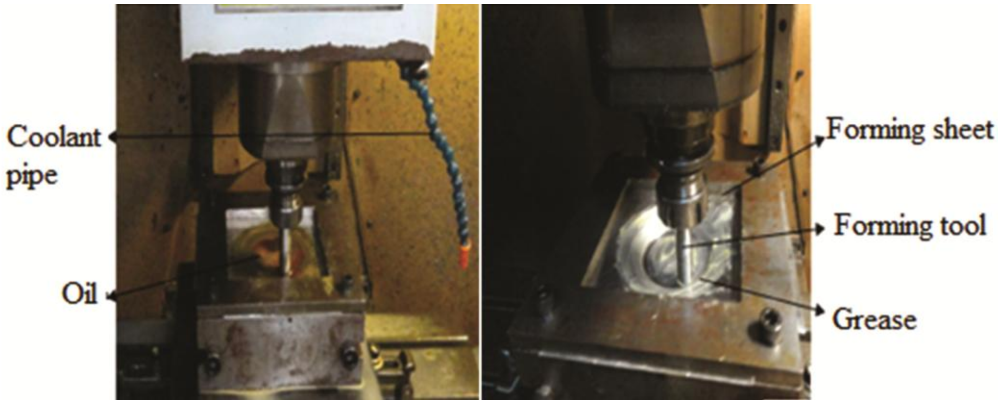

Fig. 4 — Experimental set-up.

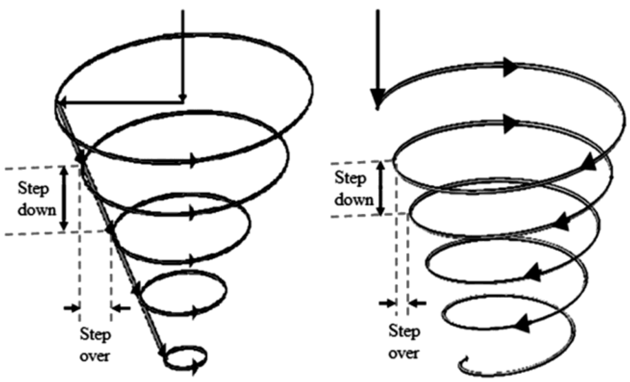

Fig. 5 — Forming tool trajectories (a) Profile and (b) Helical[5].

at the middle. The percentage of thickness reduction was taken into account for this purpose.

2.3 Process parameters and design of experiment

In this study, seven input variables (tool path, tool diameter, sheet thickness, step size, spindle speed, feed rate, and lubrication) have been investigated for optimization of forming force and thickness reduction on AA2014 sheets. Table 3 shows the varied parameters with their respective levels. TM has been implemented as a DOE and optimizing technique. A suitable Orthogonal Array (OA) is responsible for selecting input variables along with their levels in TM. In this study, Minitab-17 software has been executed for statistical analysis to perform TM as a DOE and ANOVA analysis. According to TM, the total number of independent comparisons for the selected factors is calculated as [2−1] + [6× (3−1)] +1=14. Degree of freedom (DOF) of OA needs to be greater than the DOF of the process (14, in this study). Therefore, mixed level OA L_{18} ($2^1 \times 3^6$) satisfies this condition and is represented in Table 4. Each experimental trial has been repeated three times in order to reduce statistical error during experimental work.

Table 2 — Characteristics of data logger system.

Model	NICTECH-3X-MTD-350/700-500
Load capacity (N)	5000
Impedance (Ω)	350±0.1
Excitation voltage (V)	5 (DC)
Power supply (V) & frequency (Hz)	220 & 50
Operating temperature range (^{o}C)	0-60
Sampling rate (samples/s)	5

Table 3 — Input parameters with their respective levels.

Sr. no.	Symbol	Input parameters	Level 1	Level 2	Level 3
1.	A	Tool Path	Profile	Helical	-
2.	B	Tool diameter (mm)	16	18	20
3.	C	Sheet thickness (mm)	1.2	2	2.3
4.	D	Step size (mm)	0.3	0.5	0.75
5.	E	Spindle speed (rpm)	0	100	200
6.	F	Feed rate (mm/min)	1500	2000	3000
7.	G	Lubrication	Coolant	Oil	Grease

3 Results and Discussion

SPIF experiments have been executed to study the impact of selected input variables on forming forces and thickness reduction. Axial peak forces have been taken into account for this purpose. Total 18 different combinations of experiments (Table 4) were carried out to get S/N ratio and mean of the axial peak forces and thickness reduction. Each combination was performed thrice in order to reduce statistical error during experimental work. Table 4 represents average values of these repetitions for axial peak force and thickness reduction. The effects of selected input factors are depicted by main effects diagrams and response tables on axial peak forces and thickness reduction. Table 5 and 6 are the response tables of means for axial peak force and thickness reduction respectively. Fig. 6 and 7 are the main effects plots of

Table 4 — Layout of L_{18} OA with response data for axial peak force (APF) and thickness reduction (TR)

Trial no. ↓	Input parameters and their levels							Mean of APF (N)	S/N ratio of APF	Mean of TR (%)	S/N ratio of TR
	A	B	C	D	E	F	G	M_{APF}	S/N_{APF}	M_{TR}	S/N_{TR}
1	Profile	16	1.2	0.3	0	1500	Coolant	1751	-64.87	38.93	-31.81
2	Profile	16	2	0.5	100	2000	Oil	2058	-66.27	51.48	-34.23
3	Profile	16	2.3	0.75	200	3000	Grease	6007	-75.57	33.88	-30.60
4	Profile	18	1.2	0.3	100	2000	Grease	1127	-61.04	47.42	-33.52
5	Profile	18	2	0.5	200	3000	Coolant	5439	-74.71	28.94	-29.23
6	Profile	18	2.3	0.75	0	1500	Oil	7203	-77.15	29.06	-29.27
7	Profile	20	1.2	0.5	0	3000	Oil	1244	-61.90	43.13	-32.70
8	Profile	20	2	0.75	100	1500	Grease	5262	-74.42	17.16	-24.69
9	Profile	20	2.3	0.3	200	2000	Coolant	7350	-77.33	29.75	-29.47
10	Helical	16	1.2	0.75	200	2000	Oil	1156	-61.26	46.89	-33.42
11	Helical	16	2	0.3	0	3000	Grease	4057	-72.16	39.87	-32.01
12	Helical	16	2.3	0.5	100	1500	Coolant	5635	-75.02	33.22	-30.43
13	Helical	18	1.2	0.5	200	1500	Grease	1185	-61.48	37.58	-31.50
14	Helical	18	2	0.75	0	2000	Coolant	2077	-66.35	47.81	-33.59
15	Helical	18	2.3	0.3	100	3000	Oil	6076	-75.67	46.55	-33.36
16	Helical	20	1.2	0.75	100	3000	Coolant	1342	-62.56	41.93	-32.45
17	Helical	20	2	0.3	200	1500	Oil	5450	-74.73	16.07	-24.12
18	Helical	20	2.3	0.5	0	2000	Grease	6310	-76.00	41.41	-32.34

means for axial peak force and thickness reduction respectively. ANOVA has been performed for recorded values of output parameters to represent the significance of input parameters (Table 7 and 8 for axial peak forces and thickness reduction respectively). Moreover, axial peak force and thickness reduction are the 'lower the better' type quality characteristic.

3.1 Response tables and response graphs

Response tables (Table 5 and 6) have been employed for experimental results for determining most influencing factors for axial peak forces and thickness reduction respectively. Delta values decide the order of the rank of input parameters. Optimal levels of impact factors are depicted by response graphs (Fig. 6 and 7). Fig. 6 and Table 5 depict that the minimum axial peak force corresponds to A_2 for tool path, B_1 for tool diameter, C_1 for sheet thickness, D_2 for step size, E_2 for spindle speed, F_2 for feed rate and G_2 for lubrication. Similarly, Fig.7 and Table 6 relates to minimum thickness reduction which corresponds to A_1 for tool path, B_3 for tool diameter, C_2 for sheet thickness, D_3 for step size, E_3 for spindle speed, F_1 for feed rate and G_3 for lubrication. The most affecting factor for axial peak force and thickness reduction can be declared using statistical rank from response tables (Table 5 and 6 respectively). Results show that the sheet thickness is most influencing factor (Table 5). For thickness reduction, the feed rate is the most influencing factor (Table 6).

Table 5 — Response table for mean (axial peak force).

Level	A	B	C	D	E	F	G
1	4160	3444	2801	4369	3784	4481	3933
2	3750	3851	4124	3655	3584	3357	3931
3	-	4570	6440	3842	4498	4028	4002
Delta	410	1126	3639	714	914	1124	71
Rank	6	2	1	5	4	3	7

Table 6 — Response table for mean (thickness reduction).

Level	A	B	C	D	E	F	G
1	35.53	40.72	42.65	36.43	40.04	28.67	36.77
2	39.04	39.56	33.56	39.30	39.63	44.13	38.87
3	-	31.58	35.65	36.13	32.19	39.05	36.22
Delta	3.51	9.14	9.09	3.17	7.85	15.46	2.64
Rank	5	2	3	6	4	1	7

3.2 Analysis of variance and residual plots

The variability of the SPIF process can be decreased by sorting the insignificant input factors from significant factors. Further, these sorted factors can be eliminated to improve the process stability. ANOVA facilitate the investigators for helping in grading the insignificant input factors by P-test. The specific parameter, owning the value of P less than 0.05, is significant for respective response of the process (in this case, forming force and thickness reduction). In addition, significance of input parameters can also be decided by values of F in ANOVA tables (Table 7 and 8). Greater the value of F, greater the significance is. Table 7 depicts that sheet thickness is the most

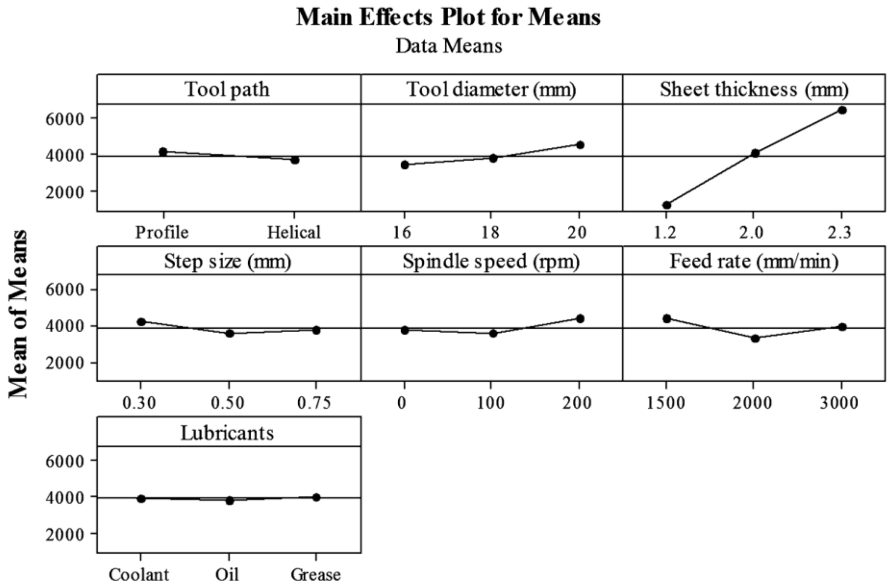

Fig. 6 — Main effects plot for means (axial peak force).

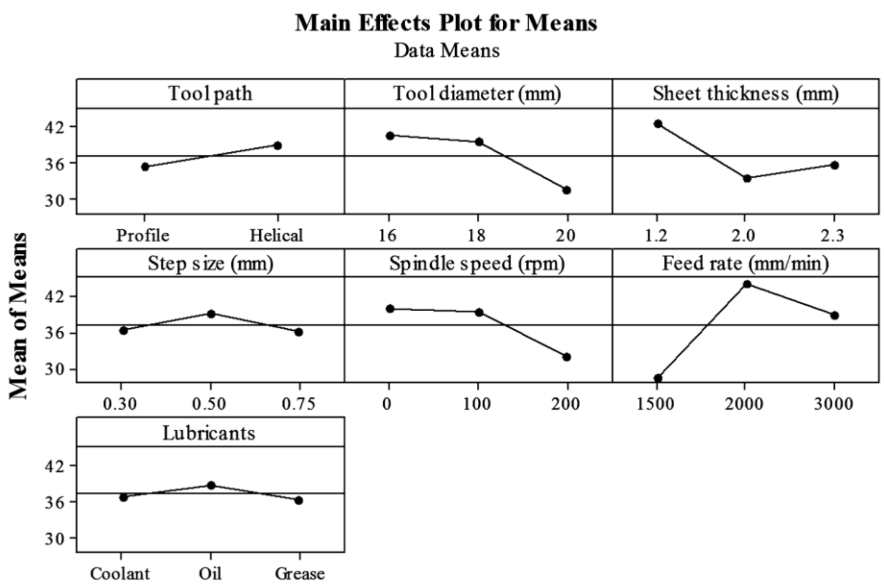

Fig. 7 — Main effects plot for means (thickness reduction).

dominating factor followed by feed rate, tool diameter, spindle speed, step size, tool path and lubrication for axial peak force, whereas, Table 8 depicts that feed rate has been most dominating factor.

Figures 8 and 9 show the four-in-one residual plot for axial peak forces and thickness reduction, respectively. The probability graph depicts the steeper angle for the residuals that stipulates the significance of process variables to experimental data. The validation of normal distribution of experimental data is confirmed for forming forces and thickness reduction by residual values as they are reclining close to straight line. Residual versus fitted values manifest the

Table 7 — Analysis of variance for axial peak forces, using adjusted SS.

Source	DF	Adj SS	Adj MS	F-Value	P-Value	% age contribution
A	1	2873175	2873175	8.96	0.005	1.00
B	2	10073575	5036788	15.71	0.000	3.53
C	2	237196707	118598353	370.00	0.000	83.26
D	2	4088906	2044453	9.38	0.004	1.43
E	2	7127019	3563509	11.12	0.000	2.50
F	2	10529454	5264727	16.42	0.000	3.69
G	2	145037	72518	0.23	0.799	0.05
Error	40	12821546	32053			4.50
Total	53	284855418				

S = 566.161, R-sq = 95.50%, R-sq (adj) = 94.04%

Table 8 — Analysis of variance for thickness reduction, using adjusted SS.

Source	DF	Adj SS	Adj MS	F-Value	P-Value	%age contribution
A	1	145.81	145.81	18.82	0.000	2.75
B	2	857.82	428.91	55.35	0.000	16.21
C	2	816.07	408.04	52.66	0.000	15.42
D	2	105.02	52.51	6.78	0.003	1.98
E	2	735.29	367.65	47.45	0.000	14.89
F	2	2227.36	1113.68	143.73	0.000	42.09
G	2	94.21	47.10	6.08	0.005	1.78
Error	40	309.94	7.75			4.85
Total	53	5291.54				

S = 2.78363, R-sq = 94.14%, R-sq (adj) = 92.24%

randomness and indecency of scattered experimental data. Residuals versus observation order graph (Fig. 8) depicts that the highest and lowest influence of input variables happened at 14th and 5th observation respectively for axial peak forces. Similarly, residuals versus observation order graph (Fig. 9) depicts that the highest and lowest influence of input variables happened at 5h and 2nd observation, respectively for thickness reduction.

3.3 Influence of process variables on response characteristics

Increase in sheet thickness and tool radius led to rise in forming forces. For a greater sheet thickness and tool radius, greater amount of material is supposed to deform

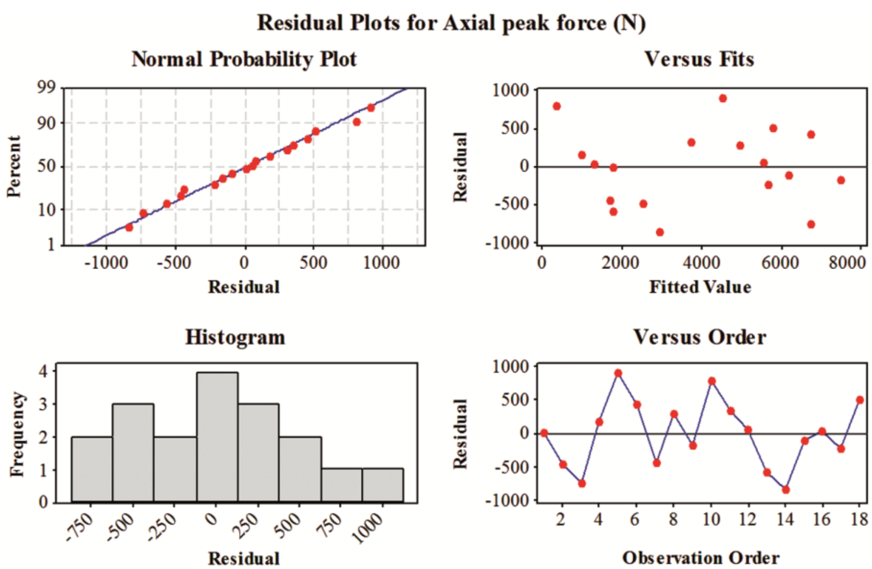

Fig. 8 — Residual plots for axial peak force.

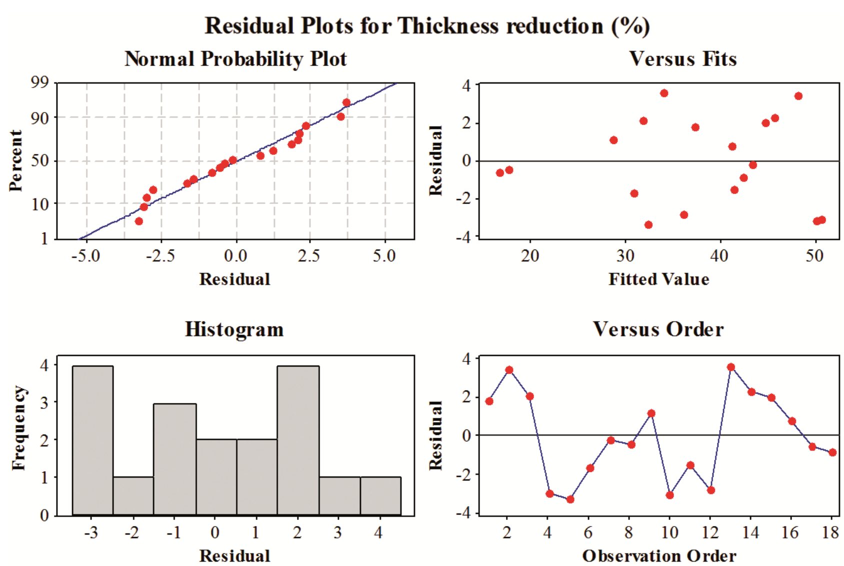

Fig. 9 — Residual plots for thickness reduction.

Table 9 — Validation of estimated results with confirmatory test.

Response	Optimal set of parameters	Predicted optimal value	Predicted CI_{CE} at 95% confidence level	Average result of three confirmatory experiments
Axial peak force	A_2, B_1, C_1, D_2, E_2, F_2 & G_2	943.98 N	$665.60 \leq \mu_{APF} \leq 1222.36$	1,127 N
Thickness reduction	A_1, B_3, C_2, D_3, E_3, F_1 & G_3	10.17 %	$4.85 \leq \mu_{TR} \leq 15.49$	14.83%

in a single pass of forming tool. Initially, forming force was decreased with the rise in step down size but started increasing gradually with the further increment in step size. It has also been observed that helical tool path formed the component with reduced forming forces. The effect of lubricants was found to be negligible on axial peak forces. Figure 7 depicts that the profile tool path results in good improvement in thickness reduction as compare to that obtained with helical tool path. Thickness reduction was decreased when a larger tool radius was employed. As spindle speed was increased, thickness reduction was found to decrease. Thickness reduction was increased initially when a higher feed rate and step size was executed.

3.4 Generating the predictive models

The optimal values of forming force and thickness reduction were recommended by response tables and graphs by providing particular levels of process variables. These levels are A_2, B_1, C_1, D_2, E_2, F_2, and G_2 for axial peak forces. Similarly, A_1, B_3, C_2, D_3, E_3, F_1 and G_3 were the optimal levels of selected parameters which correspond to optimal thickness reduction. The confidence intervals are estimated for optimal values of axial peak force and thickness reduction. In addition, optimal values are validated with values obtained by confirmatory experiments.

For calculated force values, the mean of the experimental data is calculated as

$$\mu = (\Sigma M_{APF})/18 = 3929.67 \text{ N} \quad \text{... (2)}$$

Where M_{APF} is the mean value of axial peak force of three repetitions for each amalgamation of process variables (Table 4). The predicted mean value of axial peak force (μ_{APF}) is calculated as,

$$\mu_{APF} = \{(A_2 + B_1 + C_1 + D_2 + E_2 + F_2 + G_2) - 6\mu\} \quad \text{... (3)}$$
$$= 3750 + 3444 + 1301 + 3655 + 3584 + 3357 + 3931 - (6\times 3929.67) = 943.98 \text{ N}$$

Where, values of A_2, B_1, C_1, D_2, E_2, F_2 and G_2 are acquired from Table 5. The confidence interval (CICE) is derived as following[29].

$$CI_{CE} = \sqrt{f\alpha\,(1, fe)\left(\frac{1}{\eta eff} + \frac{1}{R}\right)Ve} \quad \text{… (4)}$$

For this case, fe = 40 (from ANOVA table for axial peak force), hence, $F\alpha$ (1, 40) = 4.08[29], Ve= Variance of error for axial peak force = 32053 (Table 7).

$$\eta_{eff} = \frac{N}{1 + \text{total degree of freedom involved in prediction of mean}} \quad \text{… (5)}$$

where, N = total number of experiments, hence, η_{eff} = (18×3)/(1+13) = 3.857

Hence,

CI_{CE} = 278.38

Hence, the confidence interval for axial peak force is $665.60 \leq \mu_{APF} \leq 1222.36$.

For measured thickness reduction values, the overall mean of experimental data is $\mu = (\Sigma M_{TR})/18$ = 37.285 %, where M_{TR} is the mean value of thickness reduction of three repetitions for each amalgamation of impact factors (Table 4). The predicted average value of thickness reduction (μ_{TR}) is calculated as,

$$\mu_{APF} = \{(A_1 + B_3 + C_2 + D_3 + E_3 + F_1 + G_3) - 6\mu\} \quad \text{… (6)}$$
$$= 233.88 - 6\times 37.285 = 10.17 \%$$

where, values of A_1, B_3, C_2, D_3, E_3, F_1 and G_3 are extracted from Table 6. The confidence interval (CI_{CE}) of thickness reduction is derived from the Eq. (4) as derived in case of axial peak force. For thickness reduction, optimal value is calculated as 10.17 % and CI_{CE} as 5.32. Hence, confidence interval for thickness reduction is $4.85 \leq \mu_{TR} \leq 15.49$.

3.5 Validation of predictive models

The additional experimental work has been carried at optimal levels of process variables on AA2014 sheets for validating the predictive models. The results of confirmatory experiments were analogized with the estimated values of forming forces and thickness reduction. Table 9 depicts that the mean values responses (taken from confirmatory experiments) lies within the confidence intervals.

4 Conclusions

This study focuses on the influence of impact factors on forming forces and thickness reduction on AA2014 alloys during SPIF process. Further, the process parameters have been optimized in terms of axial peak force and thickness reduction using TM and ANOVA. The results showed that minimum axial peak force (1127 N in this case) was observed at experimental trial no. 4 when a tool of 9 mm radius was used with grease as a lubricant at 100 rpm tool rotation on 1.2 mm thick sheet, whereas maximum axial peak force was observed at trial 9 (7350 N in this case) when a tool of diameter 20 mm was employed with coolant as a lubricant at 200 rpm tool rotation on 2.3 mm thick sheet. Optimization of impact factors using TM led to following conclusions:

(i) Larger tool radius and sheet thickness lead to increment in forming forces. Helical tool trajectory is favorable to the successful forming the parts during this process. On the other hand, profile tool trajectory results in instability of required forces. The effect of selected lubricants was found to be negligible. Hence, lower sheet thickness and tool diameter can be used with helical tool path to employ smaller machinery. Thickness reduction decreases when higher tool radius and tool rotation are employed. Profile tool path and higher sheet thickness resulted in lower thickness reduction.

(ii) A helical tool path, tool radius of 8 mm, sheet thickness of 1.2 mm, step size of 0.5 mm, tool rotation of 100 rpm and feed rate of 2000 mm/min result in optimum parametric condition for optimal axial peak forces, whereas a profile tool path, tool radius of 10 mm, sheet thickness of 2.0 mm, step size of 0.75 mm, sheet thickness of 0.8 mm, tool rotation of 200 rpm, feed rate of 1500 mm/min and grease as a lubricant result in optimum parametric condition for optimal thickness reduction.

(iii) According to ANOVA statistical analysis, for axial forming forces, the most significant impact factor is sheet thickness having contribution of 83.26 % followed by feed rate (3.69 %), tool diameter (3.53 %), spindle speed (2.50 %), step size (1.43 %), tool path (1.00 %) and lubricant (0.05 %), whereas for thickness reduction, the most significant process variable is feed rate having contribution of 42.09 %.

(iv) Confirmation tests depicted that the axial peak force and thickness reduction were within the confidence interval and close to estimated results. Response characteristics were estimated by the proposed statistical model successfully and efficiently.

(v) The statistical model for estimating the forming force and thickness reduction for the components produced by SPIF process can be put forth to production engineer to execute this die-less process for various sheet materials. In addition, the resulted guidelines for the process variables and response characteristics have capacity trigger the next revolution in the field of ISF. Future work seeks the analysis of dimensional accuracy and strain developed during ISF process.

Conflict of Interest

Authors have no conflict of interest.

References

1 Ajay & Mittal R K, Incremental Sheet Forming Technologies: Principles, Merits, Limitations, and Applications, (CRC Press, Taylor and Francis, US), 2020.
2 Li P, He J, Liu Q, Yang M, Wang Q, Yuan Q & Li Y, *Aerosp Sci Technol*, 63 (2017) 132.
3 Kumar A, Gulati V, Kumar P, Singh V, Kumar B & Singh H, *J Mater Res Technol*, 1 (2019) 1461.
4 Kurra S, Regalla S P & Pérez-Santiago R, *Adv Mater Process Technol*, 1 (2015) 201.
5 Kumar A, Gulati V, Kumar P & Singh H, *J Braz Soc Mech Sci & Eng*, 41 (2019) 251.
6 Kumar A & Gulati V, *Measurement*, 131 (2019) 419.
7 Kumar A, Gulati V & Kumar P, In Advances in Industrial and Production Engineering, (Springer, Singapore), (2019) 423.
8 Kumar A, Gulati V & Kumar P, *Mater Today: Proc*, 14 (2018) 28026.
9 Ambrogio G, Filice L, Fratini L & Micari F, Some relevant correlations between process parameters and process performance in incremental forming of metal sheets, *In Proceedings of the 6th Esaform Conference on Material forming*, 2003, 175.
10 Kim T J & Yang DY, *Int J Mech Sci*, 42 (2000) 1271.
11 Ham M & Jeswiet J, *CIRP Ann Manuf Technol*, 55 (2006) 241.
12 Duflou J R, Callebaut B, Verbert J & De Baerdemaeker H, *CIRP Ann Manuf Technol*, 56 (2007) 273.
13 Aerens R, Eycken, P, Van Bael A & Duflou J R, *Int J Adv Manuf Tech*, 46 (2010) 969.
14 Oleksik V, Pascu A, Gavrus A & Oleksik M, *Academic J Manuf Eng*, 8 (2010) 51.
15 Bagudanch I, Garcia-Romeu M L, Centeno G, Elías-Zúñiga A & Ciurana J, *J Mater Process Technol*, 219 (2015) 221.
16 Centeno G, Bagudanch I, Martínez-Donaire A J, Garcia-Romeu M L & Vallellano C, *Mater Design*, 63 (2014) 20.
17 Kumar A, Gulati V & Kumar P, *Int J Eng Technol*, 10 (2018) 680.
18 Kumar A & Gulati, *Sādhanā*, 43 (2018) 159.
19 Petek A, Kuzman K & Kopač J, *Arch Mater Sci Eng*, 35 (2009) 107.
20 Duflou J, Tunckol Y, Szekeres & Vanherck A P, *J Mater Process Technol*, 189 (2007) 65.
21 Ambrogio G, Filice L, Gagliardi F & Micari F, *Adv Mat Res*, 6 (2005) 479.
22 Young D & Jeswiet J, *Proc Inst Mech Eng B J Eng Manuf*, 218 (2004) 1453.

23 Skjødt M, Bay N, Endelt B & Ingarao G, *Int J Mater Form*, 1 (2008) 1199.
24 Hussain G & Gao L, *Int J Mach Tools Manuf*, 47 (2007) 419.
25 Gulati V, Aryal A, Katyal P & Goswami A, *J Inst Eng (India): Series C*, 97 (2016) 185.
26 Kurra S & Regalla S P, *J. Mater Res Technol*, 3 (2014) 158.
27 Kumar A, Gulati V & Kumar P, *Procedia Comput Sci*, 133 (2018) 1014.
28 Gulati V & Kumar A, *Int Res J Eng Tech*, 4 (2018) 784.
29 Ross P J, Taguchi Techniques for Quality Engineering (McGraw-Hill Book Company, Singapore), 1998.